Toward Homochiral Protocells in Noncatalytic Peptide Systems

Marcelo Gleiser · Sara Imari Walker

Abstract The activation-polymerization-epimerization-depolymerization (APED) model of Plasson et al. has recently been proposed as a mechanism for the evolution of homochirality on prebiotic Earth. The dynamics of the APED model in two-dimensional spatially-extended systems is investigated for various realistic reaction parameters. It is found that the APED system allows for the formation of isolated homochiral proto-domains surrounded by a racemate. A diffusive slowdown of the APED network induced, for example, through tidal motion or evaporating pools and lagoons leads to the stabilization of homochiral bounded structures as expected in the first self-assembled protocells.

Keywords Homochirality · Prebiotic chemistry · Abiogenesis · Protometabolism · Proto-cells

Introduction

While much progress has been made in understanding the many aspects related to the origin of terrestrial life, a coherent framework of events leading up to first life is still beyond reach. Current theories of the origin of life typically address one of its aspects. For example, investigations may focus on prebiotic chemistry as in the Miller experiment (Miller 1955) and related follow-up studies (Rode 1999) or on the formation of the first cellular membranes as in the work of Deamer and collaborators (Deamer et al. 2002; Morowitz et al. 1988). Here we attempt to combine a recent scenario for the onset of homochirality in peptide systems with models describing the formation of localized cell-like proto-domains in an effort to synthesize some of the ideas presented in the literature into a cohesive framework.

M. Gleiser (✉) · S. I. Walker
Department of Physics and Astronomy, Dartmouth College, Hanover, NH 03755, USA
e-mail: gleiserm@gmail.com

A critical step in the emergence of life was the advent of cellular membranes. Membranous boundaries are a key component of all modern cells and are required for processes such as speciation, energy capture, and metabolic catalytic reactions (Monnard and Deamer 2002). "Minimum protocells"—membrane vesicles capable of self-replication—have been proposed by Morowitz et al. as a possible first step toward functioning cells fitted for self-replication and Darwinian evolution (Morowitz et al. 1988). The appeal of this membrane-first, lipid-world scenario is the ability of such boundary structures to thermodynamically separate their contents from the external environment: the interior of the membrane provides a closed microenvironment for chemical reactions while the exterior environment provides free energy and nutrients (Morowitz et al. 1988). This view is supported by numerous studies focusing on the formation of lipid membrane-vesicles from prebiotically relevant ingredients: vesicle formation has been demonstrated for a variety of amphiphilic compounds (Deamer 2002; Deamer and Dworkin 2005; Monnard and Deamer 2002, Lonchin et al. 1999; Berclaz et al. 2001a, b including formation of boundary structures from organic molecules found in the Murchison meteorite (Deamer 1985).

In contrast to the perspective provided by proponents of the lipid-world scenario (Segrè et al. 2002), self-organization of short peptides has recently been proposed as a possible alternative to lipid self-organization for formation of the first protocellular membrane structures (Fishkis 2007; Santoso et al. 2002). Although phospholipids are the primary components of modern cellular membranes, it is unlikely that such compounds were prevalent enough on the early Earth to be major components of the very first membranes (Deamer et al. 2002; Lazcano and Miller 1996). As pointed out by Fishkis (2007), the first cellular membranes may have consisted of polypeptides, possibly in conjunction with other prebiotic amphiphilic molecules. This idea is supported by findings indicating that short peptides can aggregate into fibrils, microtubes, and vesicles (Reches and Gazit 2004, 2006; Santoso et al. 2002; Vauthey et al 2002).

The notion of a "peptide-first" origin of life where polypeptides self-organize into protocellular structures is not new. Earlier work by Fox and coworkers (Fox 1973, 1980) addressed the formation of proteinoid microspheres from self-organizing amino acids. It was found that heated amino acids can self-order in copolymerization reactions and self-organize when in contact with water to form protocells (also referred to as minimal or pre-contemporary cells (Fox 1973)). These protocells can feature many of the properties common to life: metabolism, growth, reproduction and response to stimuli in the environment (Fox et al. 1995). They are also capable of evolving to more modern cells—including the initiation of a nucleic acid coding system (Fox et al. 1995). However, the polypeptides in these studies are composed of mixed *L*- and *D*-amino acids with no mention of how a microsphere might evolve toward a homochiral contemporary cell with exclusively *L*-amino acids (Fox 1973).

Apart from studies of the origins of the first cellular boundaries, the origin of life's chiral signature, *i.e.* dextrorotatory sugars and levorotatory amino acids, has been a longstanding question in studies of abiogenesis (Bonner 1996). The first breakthrough in understanding biomolecular chiral symmetry-breaking occurred with the influential work of Frank (1953), where autocatalysis and some form of mutual antagonism were identified as sufficient ingredients for obtaining molecular homochirality. Since then, many "Frank models" have been proposed, each

providing its own description of chiral symmetry breaking. These models range from the early work on bifurcation models by Kondepudi and Nelson (1983) and Avetisov and Goldanskii (1993) to more recent investigations of crystallization (Saito and Hyuga 2005; Viedma 2005), and chiral selection in polymerization (Sandars 2003; Saito and Hyuga 2005). One of the better known models is that of Sandars (2003); Brandenburg and Multamäki (2004); Wattis and Coveney (2005); Gleiser and Walker (2008), where the mutual antagonism is provided by enantiomeric cross-inhibition in template-directed polycondensation of polynucleotides (Joyce et al. 1984). Although this model provides a theoretically elegant description of how homochirality might emerge in a RNA world, the autocatalytic reactions necessary for chiral symmetry breaking to be observed in such a system are presently only demonstrated for a few non-biological molecules (Blackmond 2004; Soai et al. 1995) and would be trying to achieve with even very simple organic molecules (Joyce 1991).

A more recent proposal, describing the emergence of homochirality in an early peptide world has been provided by Plasson et al. (2004). A prebiotically relevant reaction network consisting of activation, polymerization, epimerization, and de-polymerization (APED) of chiral peptides was shown to allow self-conversion of all chiral subunits to a single handedness. As discussed by Plasson et al., and later by Brandenburg et al. (2007), the APED model is distinct from the class of Frank models in that symmetry breaking in APED *mimics* autocatalysis without any of the molecules actually possessing catalytic behavior. The APED system therefore represents what may be the first in a class of models which are not dependent on autocatalysis—a beneficial feature given that direct autocatalysis is not believed to be possible with short nucleotides or short peptides (Brandenburg et al. 2007).

Another attractive feature of the APED model is that it describes a mass-conserving, closed, recycled system of reversible chemical reactions allowing complete conversion of all chiral subunits to a single chirality: in other words, with continual input of energy, the APED system provides a description of *emergent* chirality, where one may begin with a closed near-racemic system of left and right-handed deactivated monomers and end with a nearly homochiral system of monomers and dimers. It is this feature that makes the model appealing—it provides a bottom-up approach to the onset of homochirality.
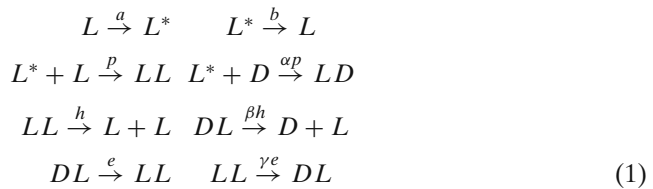
A bottom-up approach to the origins of life, based on increased complexification from primordial prebiotic precursors (Frank 1953; Miller 1955; Lazcano and Miller 1996; Avetisov and Goldanskii 1993; Sandars 2003; Brandenburg and Multamäki 2004; Gleiser and Walker 2008; Rode 1999) is usually contrasted with top-down methods aimed at reducing cells to the minimal ingredients necessary to still be deemed living (Rasmussen et al. 2004; Szostak et al. 2001). Although there is no doubt that both approaches are fundamentally sound and worth pursuing, very little work has been done in trying to bridge the gap between the two, that is, in trying to go from chemistry to biology. Our goal in the present manuscript is to take the first steps in this direction, by providing a workable closed chemical model which evolves dynamically through its own self-interactions towards precursors of cell-like homochiral structures surrounded by a racemic environment. By "cell-like" we mean spatially-bounded structures with contents differentiated from the exterior and with a hint of proto-metabolic activity. We do not attempt here to model full cell-like behavior, including transmembrane ionic transport activity and division with transmission of genetic information. Our goal is to provide the possible first

steps toward more complex and realistic cell-like behavior including homochiral biochemistry.

For this end, we will introduce spatial dynamics to the APED model and obtain the reaction rates allowing for the emergence of localized homochiral domains. We will see that both tube-like and spherical domains are possible, depending on the details of the dynamics. We begin our discussion with a description of some of the key features of the APED model in the section "The Model". We then introduce spatial dynamics and discuss our findings in the "Results" section. In the "Discussion" we make contact with proto-cellular abiogenesis in light of the work by Fox and colleagues (Fox 1973, 1980; Fox et al. 1995) and by Fishkis (2007), highlighting peptides as a potentially crucial ingredient in the first protocells. We also briefly discuss the consequences of our work to future searches of extraterrestrial stereochemistry.

The Model

The polymerization reactions in the original work of Plasson et al. were limited to dimerizations (Plasson et al. 2004): a relevant truncation given that dipeptides have been identified in the Murchison meteorite (Meierhenrich et al. 2004). We follow this simplification here, since solving the coupled network of reaction equations becomes quite complex when spatial dynamics are included. The set of APED reactions limited to dimerizations is:

$$L \xrightarrow{a} L^* \qquad L^* \xrightarrow{b} L$$
$$L^* + L \xrightarrow{p} LL \quad L^* + D \xrightarrow{\alpha p} LD$$
$$LL \xrightarrow{h} L + L \quad DL \xrightarrow{\beta h} D + L$$
$$DL \xrightarrow{e} LL \qquad LL \xrightarrow{\gamma e} DL \qquad (1)$$

supplemented by the complementary reactions with $L \leftrightarrow D$. By convention (Plasson et al. 2004), the reacting amino acid is on the left side of a polymer chain. Here a and b are the activation and deactivation rates of monomers, respectively. The rates p and h describe the respective rates of polymerization and depolymerization of homochiral dimers, while e describes the rate of epimerization of heterochiral dimers. The rates αp, βh, and γe then correspond to the complementary stereospecific reactions rates for polymerization and depolymerization of heterochiral dimers and epimerization of homochiral dimers, respectively, where α, β, and γ quantify the degree of stereoselectivity. An important feature of the model is that the system is closed with respect to mass flux and maintains a constant total concentration of amino acids and peptides,

$$c \equiv [L] + [D] + [L^*] + [D^*] + 2([LL] + [DD] + [LD] + [DL]) . \qquad (2)$$

Successful symmetry breaking in APED systems requires stereospecific reactions, i.e., $\alpha, \beta, \gamma \neq 1$. Studying the case of complete stereoselectivity for depolymerization and epimerization reactions ($\beta = \gamma = 0$), Plasson et al. found that the system allows four types of fixed points, labeled asymmetric, symmetric, dead, and unstable. The behavior of the system is thus governed by the nonzero stereoselectivity parameter,

α, and the conserved total mass through the parameter c. Together, these two parameters control the type of fixed point. In *all* cases, if c is below a critical value, no dimers ever form. This is the (racemic) dead solution. The existence of these low concentration dead solutions becomes important when we study spatially extended systems. A stereoselectivity favoring formation of homochiral dimers ($\alpha < 1$) was found to be essential in producing stable homochiral solutions (Brandenburg et al. 2007; Plasson et al. 2004) even in the relevant case of increased stereoselective pressure due to the presence of nonzero β and γ. Therefore, in this work we will restrict our investigations to the case $\alpha < 1$.

As pointed out by Plasson et al., the model can be applied to realistic systems of amino acid derivatives (Plasson et al. 2004). Although amino acids have been shown to be synthesized under a variety of prebiotically relevant conditions (Miller 1955; Rode 1999), this fact alone is not enough to guarantee the eventual emergence of peptide chemistry or life: free amino acids are notoriously poor reactants. Therefore, the limiting factor in primitive peptide synthesis is most likely *not* the formation of the amino acids but, instead, their eventual activation.

The most commonly cited potential prebiotic activations of stable amino acid derivatives lead to the formation of N−carboxyanhydrides of α-amino acids (Commeyras et al. 2002; Huber and Wächtershäuser 1998; Leman et al. 2004). NCAs have several features that make them highly amenable to building a desirable prebiotic chemistry (*i.e.* a *homochiral* chemistry) based on the APED set of reactions (Plasson et al. 2004):

1. NCAs are very reactive amino acid derivatives, which easily permit the formation of peptides in aqueous solutions.
2. The polymerization of NCAs is stereoselective, favoring the formation of homochiral peptides.
3. The chemistry of NCAs promotes the recycling of products.

There exists a wide range of models based on the chemistry of NCAs with different energy sources for activation. Potential compounds that may have acted as sources of energy to activate amino acids on the primitive Earth include nitrogen oxides, as in the primary pump model of Commeyras and coworkers (Boiteau et al. 2001; Commeyras et al. 2002); CO, familiar from the work of Wächtershäuser and collaborators (Huber and Wächtershäuser 1998; Huber et al. 2003; Wächtershäuser et al. 1992); or COS, as in the model of Leman et al. (2004). Such sources of chemical energy would have existed on the early Earth, possibly in large quantities due to increased geological activity during the Hadean era such as outgassing from volcanos. For a NCA-driven APED chemistry, these activating compounds provide the necessary free energy required for the system to have operated in a primordial environment (Plasson et al. 2004; Plasson and Bersini 2008).

Results

The introduction of spatial dependence permits the net enantiomeric excess (*ee*) to evolve in space as well as time, thereby unveiling new and interesting dynamics in the APED system. We establish a spatiotemporal reaction-diffusion network from the rate equations derived from Eq. 1 by following the usual procedure in

the phenomenological treatment of phase transitions outlined below. Systems with either spatially homogeneous and inhomogeneous concentrations are investigated separately.

Introducing Spatial Dependence

Spatial dependence was introduced following the usual procedure in the phenom-enological treatment of phase transitions (Gunton et al. 1983; Langer 1992) by rewriting total derivatives as $d/dt \rightarrow \partial/\partial t - k_{1,2}\nabla^2$ in the rate equations derived from Eq. 1. This established a reaction-diffusion network with diffusion constants k_1 and k_2 describing the molecular diffusion of monomers and dimers respectively. It is convenient to introduce the dimensionless diffusion constants $\kappa_{1,2} = k_{1,2}/\kappa$, where κ is a dimensionful diffusion rate which we scale out of the network equations (typically we set $\kappa_1 = 2\kappa_2$). Some values of physically relevant diffusion rates are $\kappa = 10^{-9}$ m^{2}s^{-1} for molecular diffusion in water and $\kappa = 10^{-5}$ m^{2}s^{-1} for air (Cotterill 2002). The corresponding rate equations were then made dimensionless by scaling all concentrations $[U]$ (with U being any monomer or dimer in the network) such that the dimensionless concentrations are written as $u = \frac{p}{a}[U]$. This allowed us to scale the reaction rate p out of the network equations and to write all other network reaction rates in terms of dimensionless ratios with a (see below). Here we have chosen a as our tunable parameter as it is dependent on activation by consumption of fuel compounds from the primordial environment and is therefore more flexible than other model parameters (Plasson and Bersini 2008). We also introduce the dimensionless time and space variables $t_0 \equiv at$ and $x_0 \equiv \sqrt{a/\kappa}\ x$. One may then recover dimensionful values for a particular choice of the rate a and the diffusion coefficient κ. The dimensionless rate equations corresponding to Eq. 1 (with $b = 0$) were found to be, with $l \equiv \frac{p}{a}[L]$, $d \equiv \frac{p}{a}[D]$, etc.:

$$\frac{\partial l}{\partial t_0} - \kappa_1\nabla_0^2 l = -l - (l^* + \alpha d^*)l + 2\eta ll + \beta\eta(ld + dl),$$

$$\frac{\partial l^*}{\partial t_0} - \kappa_1\nabla_0^2 l^* = l - (l + \alpha d)l^*,$$

$$\frac{\partial ll}{\partial t_0} - \kappa_2\nabla_0^2 ll = l^* \cdot l - \eta ll + \varepsilon(dl - \gamma ll),$$

$$\frac{\partial ld}{\partial t_0} - \kappa_2\nabla_0^2 ld = \alpha l^* \cdot d - \beta\eta ld - \varepsilon(ld - \gamma dd), \tag{3}$$

and the corresponding four equations obtained with $l \leftrightarrow d$. The dimensionless reaction rates η and ε are defined as $\eta \equiv h/a$ and $\varepsilon \equiv e/a$ and ∇_0^2 is the dimensionless Laplacian (in 2d, $\nabla_0^2 = \partial^2/\partial x^2 + \partial^2/\partial y^2$). For the work presented here we have chosen values of κ_1 and κ_2 such that $\kappa_1 = 2\kappa_2$.

We also note that the global ee, defined by Plasson et al. as a measure of the net asymmetry, is given by

$$ee = ([L] + [L^*] + 2[LL] - [D] - [D^*] - 2[DD])/c\,, \tag{4}$$

where c is given in Eq. 2. The net enantiomeric excess we cite in this work is then found by spatial averaging, *i.e.*,

$$\langle ee \rangle = (1/A) \int (ee) d^2 x \,, \tag{5}$$

where A is the area.

Numerical Simulations with Stochastic Initial Conditions

The numerical implementation utilized a finite-difference leapfrog algorithm with spatial step $\delta x = 0.2$ and temporal step $\delta t = 0.005$. Periodic boundary conditions were adopted on a 512^2 square lattice in two dimensions. Near-racemic initial conditions were prepared in a two step process. First, a racemic lattice configuration was established using the analytic form of the symmetric steady-state solution to the network equations in Eq. 3 (with $b = 0$), found as a function of the total concentration c, given in Eq. 2. The dependence of the analytic solution on the total mass allowed us to use the distribution of $c(\mathbf{x})$ over the lattice to determine whether we would study a homogeneous or inhomogeneous system. For homogeneous systems, we set a uniform concentration $c(\mathbf{x}) = \langle c(\mathbf{x}) \rangle > c_{\mathrm{crit}} = 1.5$ such that symmetry breaking would be observed everywhere in the system (here c_{crit} is given for the case $\alpha = 0.35$). For inhomogeneous systems, initial high concentration regions (*i.e.* regions where $c > c_{\mathrm{crit}}$), or bubbles, were established with Gaussian profiles such that $c(\mathbf{x}, 0) = \mathcal{C} \exp[-(x^2 + y^2)/R^2]$ where $\mathcal{C}$ is the total concentration of amino acids and peptides at the bubble's core ($\mathcal{C} > c_{\mathrm{crit}}$), and R is the radius of the bubble. Outside of the bubbles, the concentration was set to zero. The final step was to create stochastic initial conditions via a generalized spatiotemporal Langevin equation. We added a Gaussian white noise term, $\xi(x, y, t)$, with zero mean and two-point correlation function $\langle \xi(\mathbf{x}', t') \xi(\mathbf{x}, t) \rangle = \theta^2 \delta(t' - t) \delta(\mathbf{x}' - \mathbf{x})$, to the rate equations. The equations of motion, $u(x, y, t)$ from Eq. 3 with the added noise terms were then solved with simple quadratic potentials, $V(u) = (1/2)u^2$ and low noise ($\theta^2 = 0.002$) until the volume-averaged enantiomeric excess achieved a steady-state Gaussian distribution centered on the racemic state. By steady-state we mean $d\langle ee(t) \rangle / dt \approx 0$, where $\langle ee \rangle$ is given by Eq. 5. Once the near-racemic initial condition was established, the noise ($\xi(x, y, t)$) was turned off and the system was then set to evolve deterministically.

Homogeneous Systems and Chiral Domains

We first consider the formation of chiral domains in systems with homogeneous concentrations (*i.e.* $c(\mathbf{x}, t) = $ constant).With a near-racemic initial distribution, a typical spatial volume $\mathcal{V} \gg \lambda^2$, where λ is the correlation length, will coarsen into domains of left and right-handed chiralities (Brandenburg and Multamäki 2004; Gleiser and Thorarinson 2006; Gleiser 2007). This occurs after a long induction period where activated monomers of both chiral species accumulate in the system. During the induction period, the *ee* (given in Eq. 4) remains small; however, once a sufficient concentration of activated monomers has been achieved we begin to observe regions of growing enantiomeric excess. Results demonstrating the evolution of $\langle ee \rangle$ are shown in Fig. 1 for a number of runs (the dashed lines in the figure correspond to the two sample systems of Fig. 2). We present data for both the

Fig. 1 Time evolution of spatially-averaged ee in homogeneous APED systems. Each *line* represents a system starting from a random near-racemic distribution ($ee(t = 0) < 0.001$) of monomers and dimers. The *two dashed lines* correspond to the systems shown in Fig. 2 (the *darker dashed line* corresponds to the top panel and the *lighter line* to the bottom panel)
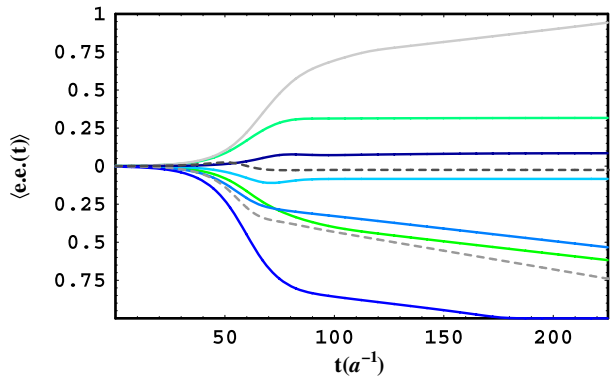
unrealistic case of complete stereoselectivity of depolymerization and epimerization reactions ($\beta = \gamma = 0$) and for more realistic nonzero parameters ($\beta, \gamma \neq 0$), although for the homogeneous systems of this section we restrict our analysis to $\beta = \gamma = 0$. We note that the results are qualitatively similar even if with realistic parameters the final *ee* never reaches a complete homochiral state (see Plasson et al. 2004). As discussed in the introduction, other polymerization models describing the onset of homochirality yield similar results for the evolution of the spatially averaged $\langle ee \rangle$ (Gleiser and Walker 2008) without the activation period which is typical of the APED model.

We have observed two types of domain evolution, as shown in Fig. 2. In the top row, domains of both chiralities percolate (*i.e.* permeate the entire volume) through the volume and the system reaches a steady-state consisting of two domains
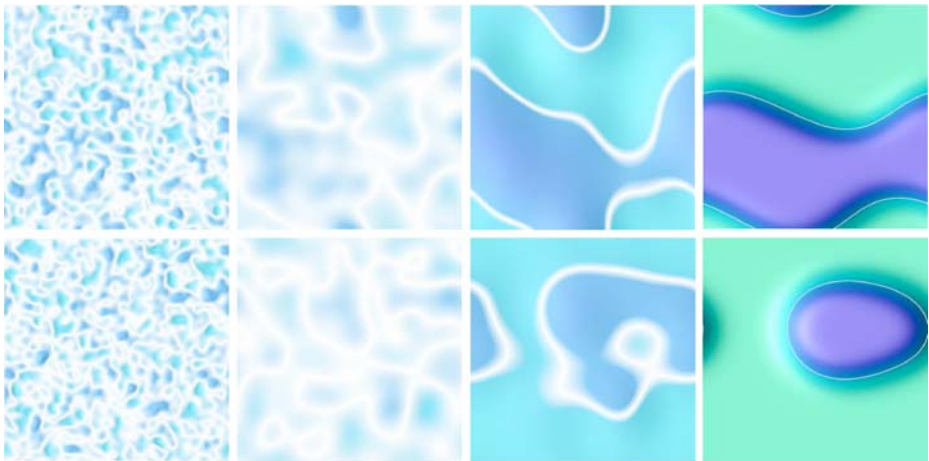
Fig. 2 Evolution of chiral domains. Time increases from left to right. *Top*. Formation of two percolating domains of opposing chirality. The phases of *L* (*dark blue*) and *D* (*aqua*) achieve near complete homochirality divided by a thin racemic (*white*) domain wall. *Bottom*. Only one domain (*aqua*) percolates and the system evolves toward a single chirality ($ee = -1$, corresponding to the homochiral *D*-phase)

with opposing chirality separated by a thin domain wall. In the bottom row, only one chiral domain percolates and the system eventually evolves toward homochirality. The parameters chosen here ($\beta = \gamma = 0$ with $\alpha = 0.3$, $\varepsilon = \eta = a$, and $b = 0$) allow for near complete conversion to homochirality: within a single domain, the net *ee* $\geq$ 99%.

Quite interestingly, the domain wall or ring-like structure surrounding the homochiral domains consists of a racemic mixture of monomers and dimers including large concentrations of the heterodimers DL and LD, as shown in Fig. 3. This is very suggestive of a physical barrier isolating the inside of the homochiral domain and is true both when only one chirality percolates (bottom-right snapshot), and when both chiralities percolate (top-right snapshot), where one observes the formation of tubular domains. These situations are suggestive of micelle vesicles and bilayer membranes, observed in emerging self-assembled structures of amphiphiles (Deamer et al. 2002). It is thus of great interest to examine the possibility of assembling similar structures in an inhomogeneous context, such that homochiral protodomains may become surrounded by a racemate.

Inhomogeneous Systems: The Role of Non-Uniform Concentration

The examples discussed thus far have maintained a uniform concentration over the entire lattice. We now consider the more realistic dynamics of systems with spatially-dependent concentrations ($c(\mathbf{x}, t) \neq$ constant). In this case, starting from stochastic near-racemic initial conditions, regions where chiral symmetry breaking occurs and regions where a racemate is maintained should emerge dynamically. Holding all reaction parameters fixed, the previous results indicate that we should observe this separation in systems where some regions have concentrations above and others below a critical, parameter-dependent value (see section "The Model"). Accordingly, our simulations show that the spatially-extended APED system naturally develops chiral protocell-like structures surrounded by a racemate, as shown in Fig. 4.

Left to evolve diffusively, the high-concentration protocellular domains containing an enantiomeric excess (Fig. 4 lower panel) would eventually shrink away. However, we must recall that in prebiotic Earth reactor pools were submitted to environmental disturbances ranging from mild (e.g. tides, evaporating lagoons) to severe (e.g. volcanic eruptions, meteoritic impacts). Both kinds of disturbances
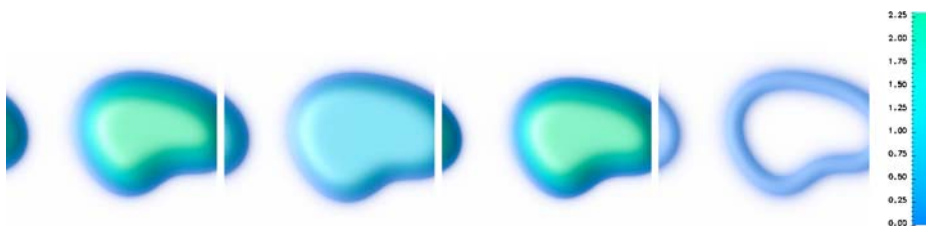
Fig. 3 Snapshots of molecular concentrations at one instant in time. From *left* to *right*, the snapshots show concentrations L, L^*, LL, and LD. *White* denotes regions where the concentration of a molecular species is < 0.15 (these regions are where an excess in D-enantiomers resides). Note that the near homochiral domain of the L-phase is surrounded by a racemic ring of LD and DL (not shown) forming a boundary around the domain
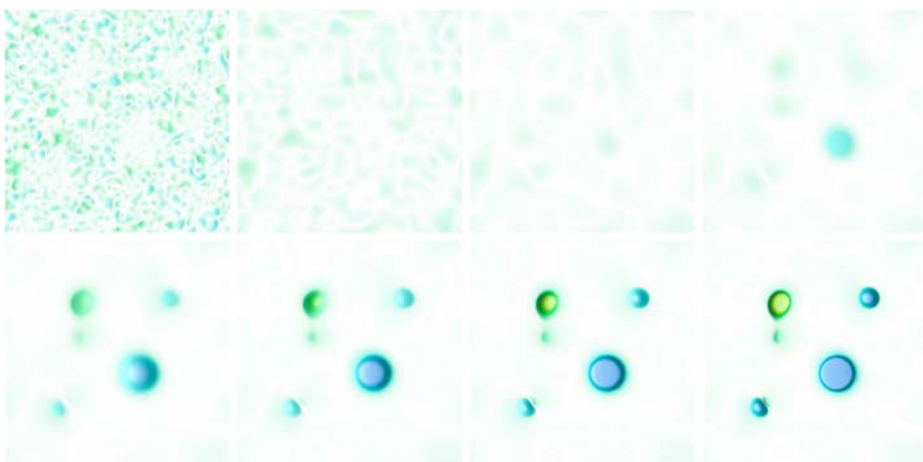
Fig. 4 Evolution of chiral protocell-like regions. Time increases from left to right and top to bottom. The diffusion was sharply decreased ($\kappa_2 = 0.1$ to $\kappa_2 = 10^{-6}$) between the top and bottom rows. *Top Row*: $t_0 = 3, 15, 45, 75$. Racemic regions (*white*) grow as activated monomers build in the system, followed by the appearance of proto-domains of chiral excess in regions where $c > c_{crit}$. *Bottom Row*: $t_0 = 135, 165, 195, 240$. The proto-domains continue to coarsen within the racemic (*white*) background as the magnitudes of the L (*dark blue*) and D (*yellow-green*) phases increase (note that since $\beta, \gamma \neq 0$, complete homochirality is not possible Ð the maximum magnitude of the *ee* in this system is $|\langle ee \rangle| = 0.6$, where $\langle ee \rangle$ is defined in Eq. 5

affected the evolution of chirality in early Earth (Gleiser et al. 2008). Recent studies of life's origins have focused on molecular interactions in the context of changing tides (Boiteau et al. 2001; Bywater and Conde–Frieboes 2005; Commeyras et al. 2002; Lathe 2004, 2005) or evaporating pools and lagoons (Robertson and Miller 1995) as ways to enhance the concentrations of reactants. From a modeling perspective, their effect can be mimicked by a time-dependent modulation in the diffusion rates.

To simulate such processes, we started the system's evolution with a fast diffusion coefficient ($\kappa_2 = 0.1$, corresponding to molecular diffusion slightly slower than that in water with dimensionful values) followed by evolution with a very slow diffusion rate ($\kappa_2 = 10^{-6}$) such as might occur for molecules diffusing on dry clay, a rocky surface, or on a beach. The initial conditions were set such that the lattice had, on average, a low concentration of amino acids and peptides: $\langle c(\mathbf{x}) \rangle < c_{crit}$, where $c_{crit} = 1.5$ for the systems studied. Bubbles with higher concentrations, $c(\mathbf{x}) > c_{crit}$, were interspersed on the lattice (see section "Numerical Simulations with Stochastic Initial Conditions"). The results of a sample run are shown in Fig. 4. The stereoselectivities have been set such that $\alpha = 0.35$, $\beta = 0.2$, and $\gamma = 0.3$ as in the "real system" parameters from Plasson et al. (2004), with the non-stereoselective reaction rates set to the dimensionless values $\varepsilon = \eta = 10$ and $b = 0$ (a and p have been scaled out of the network equations - see section "Introducing Spatial Dependence"). Since the epimerization rate on the N-terminal is of the same order as the hydrolysis rate for NCAs (Plasson et al. 2004), we have set $\varepsilon = \eta$ (*i.e. e = h*).

The top left snapshot in Fig. 4 shows a near-racemic distribution with regions of higher reactant concentration barely visible. In this simulation, the tide would ebb or the lagoon evaporate between the two leftmost snapshots in the bottom

row. Following the drying of the tidal pool or lagoon, regions with total reactant concentration initially above critical are seen to coarsen into domains with high $\langle ee \rangle$ surrounded by a near-racemic environment.

As with the homogeneous case, we also investigated if the near-homochiral domains were surrounded by a ring-like structure rich in heterodimers LD and DL. In Fig. 5, we see that, indeed, such rings do appear. The net concentrations are sensitive to the parameters β and γ and tend to be suppressed for high values. The figure shows a simulation with the values $\beta = 0.001$ and $\gamma = 0.001$. Also, as in Fig. 4, the diffusion was sharply reduced to simulate a tidal ebb: in this case, the tide would ebb prior to the snapshots shown in Fig. 5. Our results show that for small nonzero values of β and γ (typically < 0.05) the near-homochiral domains are surrounded by racemic boundary structures.

Toward Smaller Protodomains

For suitable choices of our tuneable parameter a—a measure of the energy input into the reactor pool, we can recover physically relevant, dimensionful values for the timescale and spatial extent. Here we focus on the inhomogeneous case as it offers a realistic example of a spatially-extended prebiotic system. Taking $a = 10^{-8}$ s^{-1} as in the real system parameters of Plasson et al., the hydrolysis rate assumes the value $h = 10a = 10^{-7}$ s^{-1} indicative of either high or low pH conditions (Plasson et al. 2004; Smith and Hanson 1998). Using the dimensionless space and time variables, $x_0 = 102.4$ and $t_0 = 225$ from the simulation, the physical space and time scales are $x = 35$ m and $t = 713$ y, respectively, not unreasonable values for a small pond that after evaporating for hundreds of years leaves chiral domains behind. Increasing a will *decrease* the physical size and timescales of the simulation. If, instead, we take $a = 10^{-6}$ s^{-1}, we obtain $x = 3.2$ m and $t = 7.1$ y, indicating faster time scales for evaporation of smaller lagoons or pools. A changing tide on the order of hours in microscopic protocellular domains is harder to achieve with presently accepted values of the reaction parameters. However, we have completed additional simulations on 128^2 square lattices using parameters $dt = 0.0001$ and $dx = 0.05$ where proto-domains with diameters of centimeters and timescales of years were achieved

Fig. 5 Snapshots of the enantiomeric excess and molecular concentrations of heterodimers at one instant in time. From *left* to *right* the snapshots show the *ee*, and the concentrations of LD and DL. The color scale for the first snapshot is the same as that for Fig. 4 (note that the near-homochiral domains achieve larger *ee* as compared to those of Fig. 4 due to the smallness of β and γ). For the second two snapshots, white denotes regions were the concentration is < 0.001

for $a = 10^{-5}\text{s}^{-1}$. Please note that these dimensions are not due to fundamental restrictions on the chemistry involved but due to the limitations of our numerical simulations.

Discussion

Our results demonstrate that for suitable parameter choices, the APED model exhibits chiral symmetry breaking leading to homochiral (or near-homochiral) domains in spatially extended systems. The results are qualitatively similar to those for other bottom-up polymerization models describing the onset of homochirality where domains of opposite chirality form and compete for dominance (Brandenburg and Multamäki 2004; Gleiser and Walker 2008), although here the model allows for the possibility of complete conversion of all chiral subunits for suitable parameter choices. A key point is that symmetry breaking in APED systems is sensitive to the total mass: processes, environmental or otherwise, which acted to accumulate prebiotic compounds would have favored the emergence of homochirality.

As discussed in the introduction, self-organization of short peptides has previously been proposed as a possible mechanism for formation of the first protocellular membranes (Fishkis 2007; Fox 1973, 1980). In the context of the results presented here, this implies that in regions where homochiral peptides are formed, one may observe spontaneous emergence of peptide vesicles. In fact, a compelling feature of polypeptide self-organization is that homochiral polypeptides have the propensity to form β-sheets while racemic mixtures will not exhibit such structural conformation (Brack 1979). For molecules consisting of homochiral and heterochiral segments, structural formation entails aggregation of stable homochiral β-sheets surrounded by less stable and disordered heterochiral segments (Brack 1979); furthermore, when subjected to mild hydrolysis, the more stable homochiral sheets are enriched by the residual fraction. These mechanisms may play a significant role in structural formation within the near-homochiral regions shown in Fig. 3. It is therefore plausible that formation of β-sheets will be enhanced in homochiral regions, consistent with favoring vesicle formation in regions with high *ee*, although there is no experimental proof of this correlation. In this scenario, homochiral, high concentration regions are preferentially selected to evolve into primitive protocellular structures.

Self-organized homochiral protocellular structures could potentially share many features in common with modern cellular life. Encapsulation of macromolecules has been discussed in the context of lipid membranes via dehydration–rehydration processes (Deamer et al. 2002); it is possible that such processes may have operated in peptide membranes as well (Fishkis 2007). Short peptides have been shown to exhibit catalytic activity under prebiotic conditions (Shen et al. 1990). In addition, a potential energy source for the protocell could be the chemical energy of activated amino acids (Fishkis 2007) that would still be present in the system at steady state. In fact, the APED model has been described as a protometabolic pattern (Plasson et al. 2004). At the very least, peptide protocells represent feasible prototypes displaying rudimentary features of modern cellular life (Fox 1973; Fishkis 2007). In light of the work presented here, this may now be extended to include homochiral protocells in the context of the APED model. We stress that our work says nothing of more complex cell behavior, such as nutrient exchange across cellular membranes and

cell division. But it does provide a framework to study the emergence of isolated homochiral domains within a promising peptide model, possibly a first step toward the formation of rudimentary cell-like structures in early Earth.

We also note that in the absence of a specific chiral bias, the net enantiomeric excess in the APED model, and in many models of chiral symmetry breaking, is random and may be attributable to amplification of stochastic fluctuations about the initial near-racemic state (Dunitz 1996) due to environmental influences (Gleiser et al. 2008) which may or may not induce turbulence (Brandenburg and Multamäki 2004). Therefore, as shown in Fig. 4, isolated regions can develop opposite chirality. This raises the possibility of having life forms of opposing chirality competing for resources on the early Earth (Brandenburg and Multamäki 2004). Extending this scenario to other potentially life-bearing planetary platforms, and consistent with the difficulties of using parity violation in the weak interactions as a consistent chiral bias (Gleiser 2007), our results suggests the existence of stereochemistry of opposing chirality, and possibly life, elsewhere in the universe (Castelvecchi 2007; Gleiser et al. 2008). It is hopeful that proposed robotic missions such as the Titan Organics Explorer, if funded, will be equipped to analyze enantioenriched organic compounds (Welch and Lunine 2001) shedding light on this fundamental question.

References

Avetisov V-A, Goldanskii V-I (1993) Chirality and the equation of the 'biological big bang'. Phys Lett A 172:407–410

Blackmond D-G (2004) Asymmetric autocatalysis and its implications for the origin of homochirality. PNAS 101:5732–5736

Boiteau L, et al (2001) Molecular origins of life: peptide prebiotic emergence and evolution through a permanent, cyclic molecular engine (the primary pump). Influence on the emergence of homochirality. In: Proc. first Eur. workshop on Exo-/Astro-biology, vol. 305.

Bonner W-A (1996) The quest for chirality. In: Cline DD (ed) Physical origin of homochirality in life, Santa Monica, California, February 1995. AIP Conference Proceedings, vol. 379. AIP, New York

Brack A, Spach G (1979) Beta-structures of polypeptides with L- and D-residues. J Mol Evol 13: 35–46

Berclaz N, Müller M, Walde P, Luisi P-L (2001a) Growth and transformation of vesicles studied by ferritin labeling and cryotransmission electron microscopy. J Phys Chem B 105:1056–1064

Berclaz N, Blöchliger E, Müller M, Luisi P-L (2001b) Matrix effect of vesicle formation as investigated by cryotransmission electron microscopy. J Phys Chem B 105:1065–1071

Brandenburg A, Multamäki T (2004) How long can left and right handed life forms coexist?. Int J Astrobiol 3:209–219

Brandenburg A, Lehto H-J, Lehto K-M (2007) Homochirality in an early peptide world. Astrobio 7:725–732

Bywater R-P, Conde–Frieboes K (2005) Did life begin on the beach?. Astrobio 5:568–574

Castelvecchi D (2007) Alien pizza, anyone? Biochemistry may have taken a different turn on other worlds. Sci News 172:107

Commeyras A, et al (2002) Prebiotic synthesis of sequential peptides on the hadean beach by a molecular engine working with nitrogen oxides as energy sources. Polymer Int 51:661–665

Cotterill R (2002) Biophysics: an introduction, J. Wiley, Chichester

Deamer D (1985) Boundary structures are formed by organic components of the Murchison car-
bonaceous chondrites. Nature 317:792–794

Deamer D, Dworkin J-P, Sandford S-A, Bernstein M-P, Allamandola L-J (2002) The first cell
membranes. Astrobio 2:371–381

Deamer D, Dworkin J (2005) Chemistry and physics of primitive membranes. Top Curr Chem 259:
1–27

Dunitz JD (1996) Symmetry arguments in chemistry. PNAS 93:14260–14266

Fishkis M (2007) Steps towards the formation of a protocell: the possible role of short peptides. Orig
Life Evol Biosph 37:537–553

Fox S (1973) Molecular evolution to the first cells. Pure Appl Chem 34:641–669

Fox S (1980) Metabolic microspheres. Die Naturwissenschaften 67:378

Fox S, et al. (1995) Experimental retracement of the origins of a protocell. J Biol Phys 20:17

Frank F-C (1953) On spontaneous asymmetric catalysis. Biochim Biophys Acta 11:459–463

Gleiser M, Thorarinson J (2006) Prebiotic homochirality as a critical phenomenon. Orig Life Evol
Biosph 36:501–505

Gleiser M (2007) Asymmetric spatiotemporal evolution of prebiotic homochirality. Orig Life Evol
Biosph 37:235–251

Gleiser M, Thorarinson J, Walker S-I (2008) Punctuated chirality. Orig Life Evol Biosph.
arXiv:astro-ph/0802.1446

Gleiser M, Walker S-I (2008) An extended model for the evolution of prebiotic homochirality: a
bottom-up approach to the origins of life. Orig Life Evol Biosph 38:293–315

Gunton J-D, San Miguel M, Sahni P-S (1983) In: Domb C, Lebowitz JL (eds) Phase transitions and
critical phenomena, vol 8. Academic, London

Huber M, Wächtershäuser G (1998) Peptides by activation of amino acids with CO on (Ni, Fe)S
surfaces: implications for the origin of life. Science 281:670

Huber M, Eisenreich W, Hecht S, Wächtershäuser G (2003) A possible primordial peptide cycle.
Science 301:938

Joyce G-F et al (1984) Chiral selection in poly(C)-directed synthesis of oligo(G). Nature 310:602

Joyce G-F (1991) The rise and fall of the RNA world. New Biol 3:399–407

Kondepudi D-K, Nelson G-W (1983) Chiral symmetry breaking in nonequilibrium systems. Phys
Rev Lett 50:1023–1026

Lazcano A, Miller S (1996) The origin and early evolution of life: prebiotic chemistry, the pre-RNA
world, and time. Cell 85:793–798

Langer J-S (1992) An introduction to the kinetics of first-order phase transitions. In: Godrèche C
(ed) Solids far from equilibrium. Cambridge University Press, Cambridge

Lathe R (2004) Fast tidal cycling and the origin of life. Icarus 168:18–22

Lathe R (2005) Tidal chain reaction and the origin of replicating biopolymers. Int J Astrobiol 4:19–31

Leman L, Orgel L, Ghadiri M (2004) Carbonyl-sulfide-mediated prebiotic formation of peptides.
Science 306:283

Lonchin S, Luisi P-L, Walde P, Robinson B-H (1999) A matrix effect in mixed phospholipid/fatty
acid vesicle formation. J Phys Chem B 103:10910

Meierhenrich UJ et al (2004) Identification of diamino acids in the Murchison meteorite. PNAS
101:9182–9186

Miller S-L (1955) Production of some organic compounds under possible primitive earth conditions.
J Am Chem Soc 77:2351

Monnard P-A, Deamer D (2002) Membrane self-assembly processes: steps toward the first cellular
life. Anat Rec 268:196–207

Morowitz H-J, Heinz B, Deamer D (1988) The chemical logic of a minimum protocell. Orig Life
Evol Biosph 18:281–287

Plasson R, Bersini H, Commeyras A (2004) Recycling frank: spontaneous emergence of homochiral-
ity in noncatalytic systems. Proc Natl Acad Sci 101:16733

Plasson R, Bersini H (2008) Energetic and entropic analysis of mirror symmetry breaking process in
recycled micro-reversible chemical system. arXiv:q-bio/0804.4834

Rasmussen S et al (2004) Transitions from nonliving to living matter. Science 303:963–965

Reches M, Gazit E (2004) Formation of closed-cage nanostructures by self-assembly of aromatic
peptides. Nano Lett 4:581–585

Reches M, Gazit E (2006) Designed aromatic homo-dipeptides: formation of ordered nanostructures
and potential nanotechnological applications. Phys Biol 3:S10–S19

Robertson M-P, Miller S-L (1995) An efficient prebiotic synthesis of cytosine and uracil. Nature
375:772–774

Rode B-M (1999) Peptides and the origin of life. Peptides 20:773–786

Saito Y, Hyuga H (2005) Chirality selection in crystallization. J Phys Soc Jpn 74:535–537

Saito Y, Hyuga H (2005) Chirality selection in open flow systems and in polymerization. J Phys Soc Jpn 74:1629–1635

Sandars P-G-H (2003) A toy model for the generation of homochirality during polymerization. Orig Life Evol Biosph 33:575–587

Santoso S, Hwang W, Hartman H, Zhang S (2002) Self–assembly of surfactant–like peptides with variable glycine tails to form nanotubes and nanovesicles. Nano Lett 2:687–691

Segrè D, et al. (2002) The lipid world. Orig Life Evol Biosph 31:119–145

Shen C, Lascano A, Oro J (1990) The enhancement activities of histidyl–histidine in some prebiotic reactions. J Mol Evol 31:445–452

Smith R-M, Hanson D-E (1998) The pH-rate profile for the hydrolysis of a peptide bond. J Am Chem Soc 120:8910–8913

Soai K, Shibata T, Morioka H, Choji K (1995) Asymmetric autocatalysis and amplification of enantiometric excess of a chiral molecule. Nature 378:767–768

Szostak J-W, Bartel D-P, Luisi P-L (2001) Synthesizing life. Nature 409:387–390

Wächtershäuser G (1992) Groundworks for an evolutionary biochemistry: the iron-sulphur world. Prog Biophys Mol Biol 58:85–201

Wattis J-A, Coveney P-V (2005) Symmetry-breaking in chiral polymerization. Orig Life Evol Biosph 35:243–273

Welch CJ, Lunine JI (2001) Challenges and approaches to the robotic detection of enantioenrichment on Saturn's moon, Titan. Enantiomer 6:69–81

Vauthey S, et al (2002) Molecular self-assmebly of surfactant-like peptides to form nanotubes and nanovesicles. PNAS 99:5355–5360

Viedma C (2005) Chiral symmetry breaking during crystallization: complete chiral purity induced by nonlinear autocatalysis and recycling. Phys Rev Lett 94:065504